Ind. J. Pharm. Edu. Res., 2025; 59(4):1534-1545.
https://www.ijper.org

Original Article

Silencing of S100A16 in Cervical Cancer Cells Inhibits Cancer Cell Growth by Inducing Autophagy via PI3K/AKT/mTOR Signaling Pathway

Haibin Zhang*, Wenhu Xing, Yufeng Li, Xianyun Xu

Department of Gynecology, the Second Hospital of Lanzhou University, Cuiyingmen, Chengguan, Lanzhou, Gansu, CHINA.

ABSTRACT

Objectives: Cervical Cancer (CC) ranks among the top 3 leading malignancies that affect the female reproductive system. This research focused on examining the impact of S100A16 silencing in HeLa and CaSki cells, alongside exploring the underlying molecular mechanisms involved. **Materials and Methods:** Cells were treated with si-S100A16 for a specific duration, as well as the impacts on migration, cell proliferation, cell cycle progression, apoptosis, as well as various signaling pathways were assessed. Additionally, *in vivo* tumor xenograft assays were carried out to evaluate the influence of S100A16 on tumor development. **Results:** The data revealed a significant rise in S100A16 expression in cervical cancer cells. Silencing S100A16 caused a considerable decrease in cell proliferation, hindered migration, enhanced apoptosis, and inhibited the PI3K/Akt/mTOR signaling pathway, while simultaneously inducing autophagy. In HeLa tumor-bearing mice, S100A16 silencing demonstrated robust anti-tumor effects by increasing the expression of autophagy-related proteins LC3II/I and Beclin1, simultaneously reducing p62 expression. Furthermore, levels of phosphorylated PI3K, Akt, as well as mTOR were markedly decreased. **Conclusion:** The study demonstrated that S100A16 silencing impairs the PI3K/AKT/mTOR signaling pathway, consequently enhancing cellular autophagy. These results underscore the anti-tumor potential of S100A16 silencing in CC cells, likely due to its suppression of the PI3K/AKT/mTOR pathway, which enhances autophagy.

Keywords: Autophagy, Cervical cancer, PI3K/AKT/Mtor, S100A16.

Correspondence:
Dr. Haibin Zhang
Department of Gynecology, the Second Hospital of Lanzhou University, No.82, Cuiyingmen, Chengguan, Lanzhou, Gansu-730013, CHINA.
Email: haibin_zhang@126.com

Received: 30-01-2024;
Revised: 13-03-2025;
Accepted: 04-07-2025.

INTRODUCTION

Cervical Cancer (CC) is identified among the three most prevalent malignancies affecting the female reproductive system, primarily caused by Human Papillomavirus (HPV) infection.[1,2] CC ranks second in incidence only to breast cancer, and is a leading cause of mortality among women.[3] It remains to present a major public health issue, especially affecting middle-aged women globally. Based on global cancer statistics for 2024, CC ranks fourth in incidence and mortality among women, with around 660,000 new cases and 350,000 deaths reported in 2022.[4] The prognosis for patients with advanced or recurrent CC remains poor, with one-year survival rates ranging between 10% and 20%. Although surgical intervention or radiotherapy, combined with adjuvant chemotherapy, has yielded satisfactory local control rates for early-stage CC,[5] these treatments still have certain limitations due to surgical trauma, side effects, and risk of recurrence. In recent years, targeted tumor therapy, as an advanced cancer treatment strategy, has brought new hope in the treatment of CC. Recent advancements in treatment, including small molecule inhibitors and monoclonal antibodies, offer some hope for the treatment of CC.[6] However, targeted therapy has some disadvantages, such as severe side effects, limited therapeutic effect of single targeted drug, high price, and most targeted drugs are not suitable for all cancer patients. Therefore, it is urgent to find new targeted genes and therapeutic regimens for the treatment of CC.

Research has confirmed that calcium-binding proteins play important biological roles in tumor proliferation, apoptosis, metastasis, and inflammation.[7,8] S100 calcium-binding protein A16 (S100A16) is part of the S100 family of calcium-binding proteins, extensively found throughout human tissues.[9] Research indicates that the overexpression of S100A16 is associated with varying rates of tumor occurrence and progression. Elevated levels of S100A16 expression in lung adenocarcinoma, ovarian cancer, CC, as well as gastric cancer correlate with adverse outcomes.[10-13] Research has demonstrated that S100A16 functions as an oncogene in various cancers, including colorectal and gastric cancers.[14-16] Furthermore, research reported that S100A16 increased the expression of Oct4 and Nanog in human CC cells,

DOI: 10.5530/ijper.20251170

suggesting it could act as an oncogene in CC.[17] Additionally, our earlier work revealed that the expression of S100A16 was considerably elevated in tumor tissue samples and was strongly associated with the cell cycle, based on a comparison of S100A16 expression in CC tumor tissues and normal tissues using the TCGA database.[12] Therefore, S100A16 may be exploited as a therapeutic target for CC. However, the regulatory mechanism of S100A16 in CC was still not fully understood.

The PI3K/Akt signaling pathway is recognized as essential in the development of numerous cancers.[18] mTOR, a key kinase involved in regulating autophagy, is part of the PI3K/Akt/mTOR pathway, which has been targeted to inhibit tumor growth.[19] Overactivation of these pathways is a significant contributor in the development of cancers, including breast cancer. In multiple types of cancers, such as CC, over-activation of the PI3K/Akt/mTOR oncogenic pathway disrupts metabolic processes, modulates apoptosis, and affects cell proliferation.[20,21] Elevated expression of this pathway has been linked to altered effectiveness of targeted therapies compared to cases with lower expression.[22] Our pervious study also reported that S100A16 could promote the proliferation, migration, and tumor angiogenesis of HeLa cells by regulating the PI3K/Akt signaling pathways.[23] Therefore, it is crucial to explore the mechanism by which S100A16 regulates the PI3K/Akt pathway in CC progression.

Autophagy, a process activated by cellular stress, is responsible for breaking down intracellular components. It is essential for preserving cellular homeostasis by directing proteins as well as organelles to lysosomes for degradation.[24,25] Autophagy plays a dual role in tumor cells, in the initial stages of tumor development, autophagy helps to slow cancer progression by reducing tissue damage and maintaining genomic stability. However, within the tumor microenvironment, increased autophagic activity often supports tumor cell survival and promotes metastasis.[26] Recent studies have shown that autophagy and abnormal expression of autophagy-related proteins are closely related to the occurrence of CC. Wang *et al.*,[27] showed that the induction of autophagy by UM-6 inhibited the viability of CC cell lines Caski and Hela and exerted an anti-CC effect. Luo *et al.*,[28] found that STIM1 could further accelerate the progression of CC by increasing TFEB nuclear translocation in CC cells and promoting autophagy. However, the regulatory mechanism by which S100A16 regulates autophagy to participate in CC progression remains unreported.

Therefore, this study was aimed to investigate the inhibitory effect of S100A16 on autophagy in CC cells and to explore the molecular mechanisms *in vitro* and *in vivo*. Furthermore, we explored the possible connection between S100A16 expression and the PI3K/Akt/mTOR signaling pathway. This study might offer a novel target and therapeutic strategy for the treatment of CC.

MATERIALS AND METHODS

Materials

RiboFect™ CP Transfection Kit was purchased from RiboBio (Cat. No. C10511-05, Guangzhou, China). Fetal Bovine Serum (FBS) (Cat. No. 10099-141) and penicillin-streptomycin (Cat. No. AE20005267) were purchased from HyClone (USA). RIPA Lysis buffer (G2002-100ML) was purchased from Servicebio (China) BCA protein assay kit was purchased from Cowin Biotech Co., Ltd. (Beijing, China). Polyvinylidene Difluoride (PVDF) membranes were purchased from Millipore (USA). The Cell Counting Kit (CCK)-8 was purchased from Biosharp Life Sciences (Anhui, China). Annexin V-APC/PI Apoptosis Detection Kit (KGA1030-100T) was from KeyGEN BioTECH (Nanjing, China). Anti-bodies Akt, Beclin1, LC3B, mTOR, P62, p-Akt, PI3K, p-mTOR, p-PI3K, S100A16, and β-actin was purchased from Abclonal (Wuhan, China), and Goat anti-rabbit IgG (H+L) was purchased from Abcam (Shanghai, China). Epoxy resin (Epon 812 Kit), uranyl acetate, and lead citrate were purchased from SPI Bio (China).

Cell lines and culture

Normal Human Cervical Epithelial Cells (HUCEC) were procured from Shanghai Yaji Biotechnology Co. Ltd. ME180 cells were sourced from Wuhan Pronosai Co. Ltd., while human cervical cancer C-33A cells were sourced from ATCC (USA). The CC HeLa cells were provided by the Shanghai Cell Bank of the Chinese Academy of Sciences, and the human cervical squamous cell carcinoma SiHa cell line was acquired from Shanghai Jikai Genetic Medicine Technology Co., Ltd. The cell lines HUCEC, ME180, C-33A, HeLa, and SiHa were kept in Dulbecco's Modified Eagle Medium (DMEM) fortified with 8%-10% FBS and 1% penicillin-streptomycin. The cultures were incubated at 37°C in a 5% CO_2 atmosphere. Cells were plated at the required density in the appropriate plates after being counted during the exponential growth phase.

Cell transfection

We silenced the expression of S100A16 using small interfering RNA (si-S100A16: Si-S100A16#1, Si-S100A16#2). To silence S100A16 expression, si-NC (5'-CAGCGAUGUAUCUCUAACCGGUUCU-3'), siRNA-S100A16#1 (CGCTTAGAAAGTGTCTTTTGTCC), and siRNA-S100A16#2 (GTGGAAAACTTCTACAAATATGT) manufactured by Shanghai Genome Pharmaceuticals were introduced into the cells. Si-S100A16#1, Si-S100A16#2, or si-NC (75 pmol/well) and transfection reagent (7.5 μL/well) were diluted in 100 μL of serum-free Opti-MEM and incubated for 5 min. The diluted transfection reagent and siRNA were then blended and incubated at 37°C for 30 min. The transfection mixture was subsequently introduced into the cell culture medium and thoroughly combined. Following a 6-hr transfection, the medium

was substituted with fresh DMEM enriched with 10% FBS, and the cells were incubated for another 48 hr.

RT-qPCR

Total RNA in CC cell lines was retrieved using the TRIzol™ Plus RNA Purification Kit (Invitrogen, USA). The Revert Aid 1st Strand cDNA Synthesis Kit (Thermo Fisher Scientific, Inc., USA) was implemented for Reverse Transcription (RT) reactions, and SYBR Green Master (Roche Molecular Systems, Switzerland) was utilized for all RT-PCR reactions. In RT-qPCR, data were interpreted as fold changes ($2^{-\Delta\Delta Ct}$) relative to the expression levels of GAPDH and U6 small nuclear RNA. PCR reaction system: 10.0 µL 2×Real PCR EasyTM Mix-SYBR, 0.8 µL Forward Primer (10 µM), 0.8 µL Reverse Primer (10 µM), 2.0µL Template (DNA), and 6.4 µL ddH_2O. The following thermal cycling conditions were implemented: 40 cycles starting with 30 sec at 95°C for predenaturation, followed by 5 sec at 95°C for denaturation, 30 sec at 55°C for annealing, 30 sec at 72°C for fluorescence collection, and 20 sec at 86°C for melting curve analysis. The sequences of the primer utilized were as follows: *GAPDH*, F: TGACTTCAACAGCGACACCCA, R: CACCCTGTTGCTGTAGCCAAA; *S100A16*, F: AAGTACAGCCTGGTCAAGAACAAGATC, R: GTGTCCGACAGCATGTGGTTCAG.

CCK-8 analysis

HeLa and SiHa cells were cultured until they reached the logarithmic phase, then treated with trypsin and prepared into a single-cell suspension using complete culture medium. A 96-well culture plate was incubated with the cell suspension in a 5% CO_2 atmosphere at 37°C for 24 hr. Once the cells had fully grown and adhered to the plate, the culture medium was discarded. The cells were then cultured for another 48 hr at 37°C in a 5% CO_2 incubator using RDA medium. After this period, each well was further incubated for 2 hr following 48 hr of drug intervention. Next, CCK-8 solution was introduced into each well. An enzyme labeling instrument was subsequently used to measure the absorbance at a wavelength of 450 nm (A). The cell proliferation rate was established utilizing the formula, and the half-maximal Inhibitory Concentration (IC_{50}) was determined. The formula for the cell proliferation rate (%) is as follows:

Cell proliferation rate (%)=drug group A/control value×100%

Flow cytometry

Flow cytometry was used to detect apoptosis in HeLa and SiHa cells. Cells were seeded into 6-well plates for 24 hr, after which transfection and hypoxia treatment were applied. The cells were treated with 0.25% trypsin (without EDTA) for 2 min using Beyotime C0205 (0.25% trypsin without EDTA). Following this, HeLa and SiHa cells were rinsed with PBS buffer and then centrifuged at 150 g for 5 min at room temperature. The cells were resuspended in 500 µL of 1×binding buffer at a concentration of 1×10^6 cells/mL and distributed into appropriate tubes at a density of 1×10^5 cells per tube. 5 µL of Annexin V-APC and 5 µL of Propidium Iodide (PI) solution were introduced to each tube, and the mixture was incubated for 15 min at room temperature in the dark. The cells were then evaluated within 1 hr utilizing a FACSCalibur™ flow cytometer (BD Biosciences, USA).

Western blot analysis

The HeLa and SiHa cell lines were lysed utilizing RIPA buffer to retrieve cellular proteins. Protein concentrations were quantified utilizing a BCA protein assay kit. Equivalent protein quantities were subjected to Sodium Dodecyl Sulfate-Polyacrylamide Gel Electrophoresis (SDS-PAGE) and subsequently moved to PVDF membranes. The membranes were incubated in a blocking solution comprising 5% skimmed milk for 2 hr, after that incubated overnight at 4°C with primary antibodies. After being rinsed with PBS, the membranes were incubated with a Horseradish Peroxidase (HRP)-conjugated secondary antibody for 2 hr at room temperature. After this incubation, the membranes were rinsed with TBST, and protein detection was performed utilizing enhanced chemiluminescence with a commercial ECL kit (Cowin Biotech Co., Ltd.), adhering to the manufacturer's guidelines. Finally, protein expression levels were measured utilizing ImageJ software (National Institutes of Health, Bethesda, MD, USA), normalizing against relative internal standards. Antibody information: Akt antibody, item no. A17909, 1:2000, Abclonal; Beclin1 antibody, item no. A17028, 1:2000, Abclonal; LC3B antibody, item no. A19665, 1:2000, Abclonal; mTOR antibody, item no. A11354, 1:2000, Abclonal; P62 antibody, item no. A19700, 1:2000, Abclonal; p-Akt antibody, item no. AP1259, 1:2000, Abclonal; PI3K antibody, item no. 4292, 1:1000, CST; p-mTOR antibody, item no. AP0115, 1:2000, Abclonal; p-PI3K antibody, item no. 17366, 1:1000, CST; S100A16 antibody, item no. A16167, 1:2000, Abclonal; β-actin antibody, item no. AC026, 1:50000, Abclonal; Goat anti-rabbit IgG (H+L), item no. ab6721, 1:5000, Abcam.

Transwell assay

Place the Matrigel in a refrigerator set to 4°C to thaw overnight. Next, dilute the Matrigel by adding three times its volume of serum-free medium. Transfer 40 mL of the diluted Matrigel solution into the upper chamber of the Transwell apparatus and incubate at 37°C for 2 hr. Adjust the cell concentration for each experimental group to 1×10^6 cells/mL and introduce 100 µL of this cell suspension into the upper chamber. Add 600 µL of serum-containing medium to the lower chamber and incubate the setup at 37°C for 48 hr. After incubation, gently remove any remaining cells on the polycarbonate membrane using a wet cotton swab. Fix the cells with formaldehyde and stain them with 0.1% crystal violet for 30 min. Lastly, randomly scan and count 5 areas using a microscope at 400× magnification and calculate the ratio against the control group.

Wound healing assay

HeLa and SiHa cells were nurtured in a 6-well plate until they achieved 80% to 90% confluence, after which a scratch assay was performed to evaluate cell migration. The Mobility Rate (MR) was determined utilizing the formula:

MR=[(initial gap at 0 h-final gap at 48 hr)/initial gap at 0 h]×100%.

Tumor xenograft assay

Twenty BALB/c nude mice, aged 6 to 8 weeks, were allocated into four groups at random (n=5 each group): shRNA-NC, shRNA-S100A16, ov-NC, and ov-S100A16, for subcutaneous xenograft tumor studies. The mice were obtained from Jiangsu Jizui Pharmachem Biotechnology Co. (SCXK(Su)2020-0004). The density of HeLa cells was set to 3.0×10^6 cells/mL, suspended in 100 µL of medium, and implanted subcutaneously into the nude mice. The construction of lentiviral vectors for over expressing S100A16 (pLJM1-S100A16-GFP) and silencing S100A16 was provided by Shanghai Hanheng Biotechnology Co., Ltd. On days 5, 8, and 11 after inoculation, the shRNA-NC group received injections of shRNA-NC encapsulated lentivirus, the shRNA-S100A16 group received shRNA-S100A16 encapsulated lentivirus, the ov-NC group received ov-NC encapsulated lentivirus, and the ov-S100A16 group received ov-S100A16 encapsulated lentivirus at the tumor site (all at a dose of 5×10^{11} virus particles). Tumor diameters were measured on days 4, 8, 12, 16, 20, and 24 post-inoculations. Twenty-four days after treatment, the mice were euthanized via cervical dislocation, and the tumors were subsequently weighed. Tumor tissue was stored at -80°C for future studies.

Detection of tumor volume and weight

Measurements were taken every four days by recording the Length (L) and Width (W) of the tumor. The volume was determined using the formula: $V=(L\times(W)^2)/2$ (V, volume; L, length diameter; W, Width diameter).

Immunohistochemical staining

Tumor tissue sections were microwaved for 20 min, then placed in 3% hydrogen peroxide at room temperature for 25 min in darkness. Sections were treated with BSA for 20 min at room temperature, followed by overnight incubation with primary antibodies (Ki67, 1:100, No. GB121141, Servicebio, China) at 4°C. After washing three times with PBS, sections were incubated with HRP-conjugated Goat Anti-Mouse IgG (H+L) (No. GB23301, 1:100, Servicebio, China) at 37°C for 30 min. DAB chromogen solution was applied for color development at room temperature, with a positive result indicated by a brownish-yellow color. Sections were stained with hematoxylin for 3 min, dehydrated in 75%, 85%, and 95% ethanol, and cleared in xylene for 10 min each. Finally, sections were mounted with neutral medium and imaged.

Transmission Electron Microscope (TEM)

Tumor tissues were initially prefixed in a 3% glutaraldehyde solution and subsequently post fixed in 1% osmium tetroxide. After fixation, the tissues underwent a series of dehydrations using acetone before being infiltrated with Epox 812 and embedded. Semithin sections were stained with methylene blue, while ultrathin sections (60-90 nm) were prepared using a diamond knife. These ultrathin sections were then stained with uranyl acetate for 10 to 15 min and lead citrate for 1 to 2 min. Finally, the sections were examined using a JEM-1400-FLASH Transmission Electron Microscope (JEOL, Japan).

Statistical Analysis

In the research, quantitative measurements are denoted as mean±Standard Deviation (SD). Statistical analysis was executed utilizing SPSS version 20.0 (IBM, USA). Sample size was determined by G*power software. An independent samples t-test was utilized to compare differences among two groups. One-way Analysis of Variance (ANOVA) was applied to assess variations across multiple groups, LSD test was used for homogeneity of variance, and Tamhane's T2 test was used for heterogeneity of variance. Statistical significance was established with a p-value of less than 0.05.

RESULTS

S100A16 was highly expressed in CC cell lines

First, S100A16 expression was assessed in normal and CC cell lines using RT-qPCR. As shown in Figure 1A, S100A16 expression was significantly increased in C-33A, HeLa, and CaSki cells (p<0.05). Subsequently, HeLa and CaSki cell lines were chosen for further experimentation. Two S100A16 knockdown models were developed, and RT-qPCR was used to detect the silencing efficiency of S100A16. The results showed that a significant reduction in S100A16 expression with si-S100A16-1# and si-S100A16-2# in both HeLa and CaSki cell lines (p<0.05) (Figure 1B). The silencing efficiency of si-S100A16-1# was 83.75±15.81%, the silencing efficiency of si-S100A16-2# was 80.93±20.84% in HeLa cells; while the silencing efficiency of si-S100A16-1# was 80.00±25.57%, and the silencing efficiency of si-S100A16-2# was 86.36±4.76 % in CaSki cells. Si-S100A16#1 and si-S100A16#2 were both efficiently silencing S100A16, confirming the successful establishment of the models. Subsequently, the si-S100A16-2# model was selected for further experimentation. In brief, the results suggested that S100A16 was highly expressed in CC cells.

Effects of S100A16 on the biological behavior of CC cells

To investigate the effect of S100A16 on the biological behavior of CC cells, S100A16 expression in HeLa and CaSki cells was evaluated utilizing RT-qPCR and Western blot methods. In comparison to the si-NC group, the si-S100A16 group showed

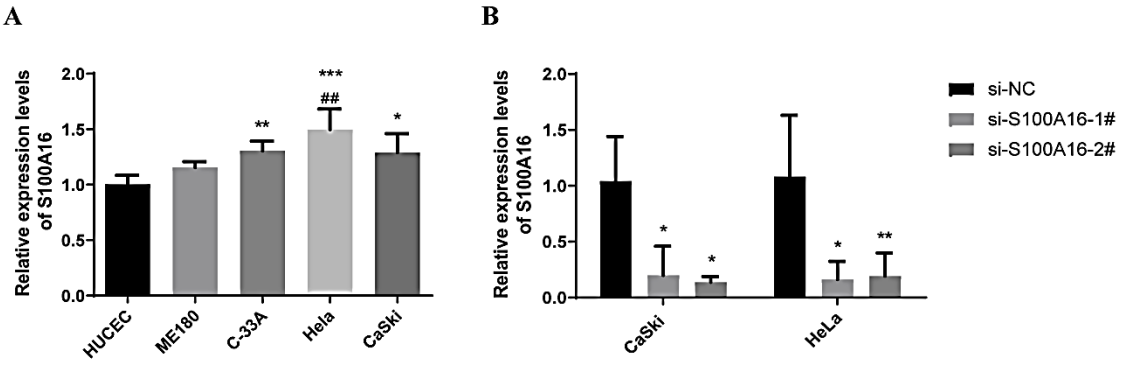

Figure 1: Expressions of S100A16 in CC cells. (A) RT-qPCR to detect the expression of S100A16 in cells. (B) RT-qPCR detection of S100A16 silencing potency. Data were shown as mean±SD (n=3). Compared with the si-NC group, $^{*}p$<0.1, $^{**}p$<0.01.

a marked reduction in S100A16 expression (p<0.05) (Figures 2A, B). CCK-8 assays subsequently indicated that the silencing of S100A16 resulted in a significant decrease in cell viability of both CaSki and HeLa cells compared to the control group (p<0.001) (Figure 2C). However, representative images from the Transwell assays showed a substantial reduction in the number of cell invasions in the si-S100A16 group both in HeLa and CaSki cell lines (Figure 2D). Quantitative analysis showed that compared with the si-NC group, the cell invasion ability of the si-S100A16 group was significantly decreased (p<0.01). Similarly, representative images from the wound healing assay showed reduced migration in the si-S100A16 group compared to the si-NC group at 24 hr post-scratch both in HeLa and CaSki cell lines (Figure 2E). Quantitative analysis of the migration distance confirmed a significant reduction in migration (p<0.001). Flow cytometry analysis further demonstrated that the percentage of cells in the G0/G1 phase was notably reduced in the si-S100A16 group relative to the si-NC group in both HeLa and CaSki cell lines (p<0.05), while the percentage of cells in the G2/M and S phases was markedly elevated in the si-S100A16 group (p<0.05) (Figure 3A). Moreover, findings from the apoptosis experiment showed a notable rise in apoptosis in the si-S100A16 group in both HeLa and CaSki cell lines (p<0.001) (Figure 3B). The percentages of apoptotic cells in Q1-LR and Q1-UR quadrants of CaSki cells in si-S100A16 group were 1.88±0.19% (Q1-LR region), 6.69±0.68% (Q1-UR region) and 8.57±0.67% (Q1-LR+Q1-UR region), respectively. The percentages of apoptotic cells in Q1-LR and Q1-UR quadrants of Hela cells in si-S100A16 group were 3.29±0.24% (Q1-LR region), 4.38±0.32% (Q1-UR region) and 7.67±0.51% (Q1-LR+Q1-UR region), respectively. These findings indicated that the inhibition of S100A16 in CC cell lines leads to reduced migration, decreased proliferative capacity, a prolonged cell cycle, and an elevated rate of apoptosis. Silencing S100A16 impairs the growth of CC cell lines, as demonstrated by these results.

Silencing S100A16 promoted autophagy by inhibiting the PI3K/AKT/mTOR signalling pathway in CC cells

Western blot analysis disclosed that the si-S100A16 group exhibited significantly reduced expression levels of p-PI3K/PI3K, p-Akt/Akt, and p-mTOR/mTOR in HeLa and CaSki cells in comparison with the si-NC group (p<0.001) (Figure 4A). Moreover, the si-S100A16 group exhibited markedly elevated levels of LC3II/I and Beclin1, while p62 expression was markedly lower (p<0.01) (Figure 4B). These results demonstrated that silencing S100A16 could suppress the activation of the PI3K/AKT/mTOR pathway, enhancing autophagy and suppressing CC cell growth.

Effects of S100A16 on the proliferation of CC cells in subcutaneous tumor-bearing mice *in vivo*

To assess the impact of S100A16 expression on cell proliferation *in vivo*, we built a subcutaneous transplant model with shRNA-S100A16 and S100A16-overexpressing HeLa cells. The representative images of the tumor were shown in Figure 5A. When contrasted with the shRNA-NC group, the shRNA-S100A16 group showed a notable reduction in tumor weight (p<0.001). Additionally, the Ov-S100A16 group had a notably greater tumor weight than the Ov-NC group (p<0.01) (Table 1). After 4, 8, 16, 20, 24 days, the tumor volumes in the shRNA-S100A16 group were notably lower as opposed to those in the shRNA-NC group (p<0.05) (Table 2). The ov-S100A16 group exhibited markedly larger tumor volumes compared to the ov-NC group on days 12, 16, and 24 (p<0.05) (Table 2). The tumor weight and volume measurements indicated that silencing S100A16 effectively inhibited CC proliferation in subcutaneous tumor-bearing mouse model. In addition, immunohistochemical analysis of Ki-67 expression in tumor tissues had considerably reduced Ki-67 levels in the shRNA-S100A16 group as opposed to the shRNA-NC group, while ov-S100A16 group exhibited notably higher Ki-67 levels than the ov-NC group (p<0.05) (Figures 5B, C). In short, silencing S100A16 effectively inhibited

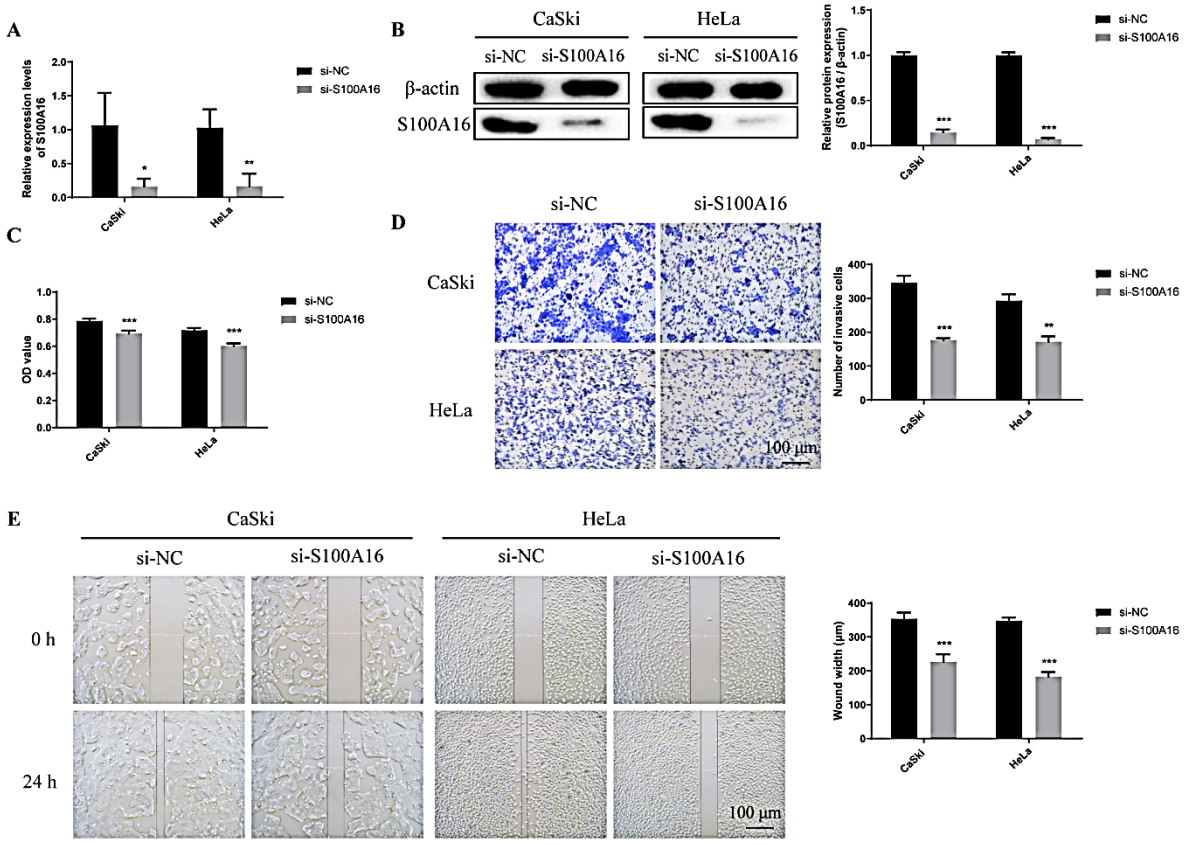

Figure 2: Effects of S100A16 on the biological behavior of CC cells. S100A16 expression was detected by RT-qPCR (A) and Western blot (B) (n=3). (C) Results of cell proliferation activity assay with CCK-8 assay (n=4). (D) Transwell assay detects the invasive capacity of each group of cells (n=3). (E) Wound healing test to determine the migration distance of each group of cells within 24 h (n=6). Data were shown as mean±SD. Compared with the si-NC group, $^{*}p$<0.1, $^{**}p$<0.01, $^{***}p$<0.001.

the proliferation of CC cells in subcutaneous tumor-bearing mice *in vivo*, while over-expression of S100A16 played an opposite role.

Effects of S100A16 on autophagy of CC cells in subcutaneous transplant tumor mouse model *in vivo*

Autophagy in tumor tissues was examined using TEM method. The shRNA-NC and ov-NC groups exhibited the presence of nuclei, normal mitochondria, rough endoplasmic reticulum, and a few autophagic lysosomes. In contrast, the shRNA-S100A16 group promoted the production of auto phagolysosomes, whereas no autophagic lysosomes were observed in the ov-S100A16 group (Figure 6A). Autophagy-associated proteins LC3II/I, P62, and Beclin1 levels in the transplanted tumors were assessed via Western blot analysis. In comparison to shRNA-NC group, the shRNA-S100A16 group displayed notable increases in LC3II/I and Beclin1 expression (p<0.001), while also demonstrating a notable reduction in P62 expression (p<0.001) (Figures 6B, C). Conversely, the ov-S100A16 group displayed a notable decrease in LC3II/I and Beclin1 levels as opposed to ov-NC group (p<0.001), while P62 expression was markedly elevated (p<0.01) (Figures 6B, C). These results demonstrated that silencing S100A16 enhanced autophagy to inhibit tumor growth, whereas overexpression of S100A16 inhibited autophagy in CC cells *in vivo*.

Effects of S100A16 on the PI3K/AKT/mTOR signaling pathway of CC cells in subcutaneous transplant tumor model *in vivo*

Simultaneously, the activity of the PI3K/AKT/mTOR signaling pathway in transplanted tumors in nude mice was assessed via Western blotting. In relation to the shRNA-NC group, the shRNA-S100A16 group displayed markedly lower expression levels of p-PI3K/PI3K, p-Akt/Akt, and p-mTOR/mTOR (p<0.001) (Figures 7A, B). In contrast, the ov-S100A16 group showed substantially higher expression levels of p-PI3K/PI3K, p-Akt/Akt, and p-mTOR/mTOR as opposed to the ov-NC group (p<0.001) (Figures 7A, B). Overall, silencing S100A16 effectively suppressed the PI3K/AKT/mTOR signaling pathway, thereby inhibiting tumor growth, while overexpression of S100A16 stimulated this pathway, leading to tumor progression *in vivo*.

DISCUSSION

CC poses a significant threat to global women's health due to its high incidence and mortality rates. Recent studies have indicated that the S100 protein family plays a crucial role in the development and progression of various malignancies, including CC. Based on our previous studies, the up-regulation of S100A16 expression

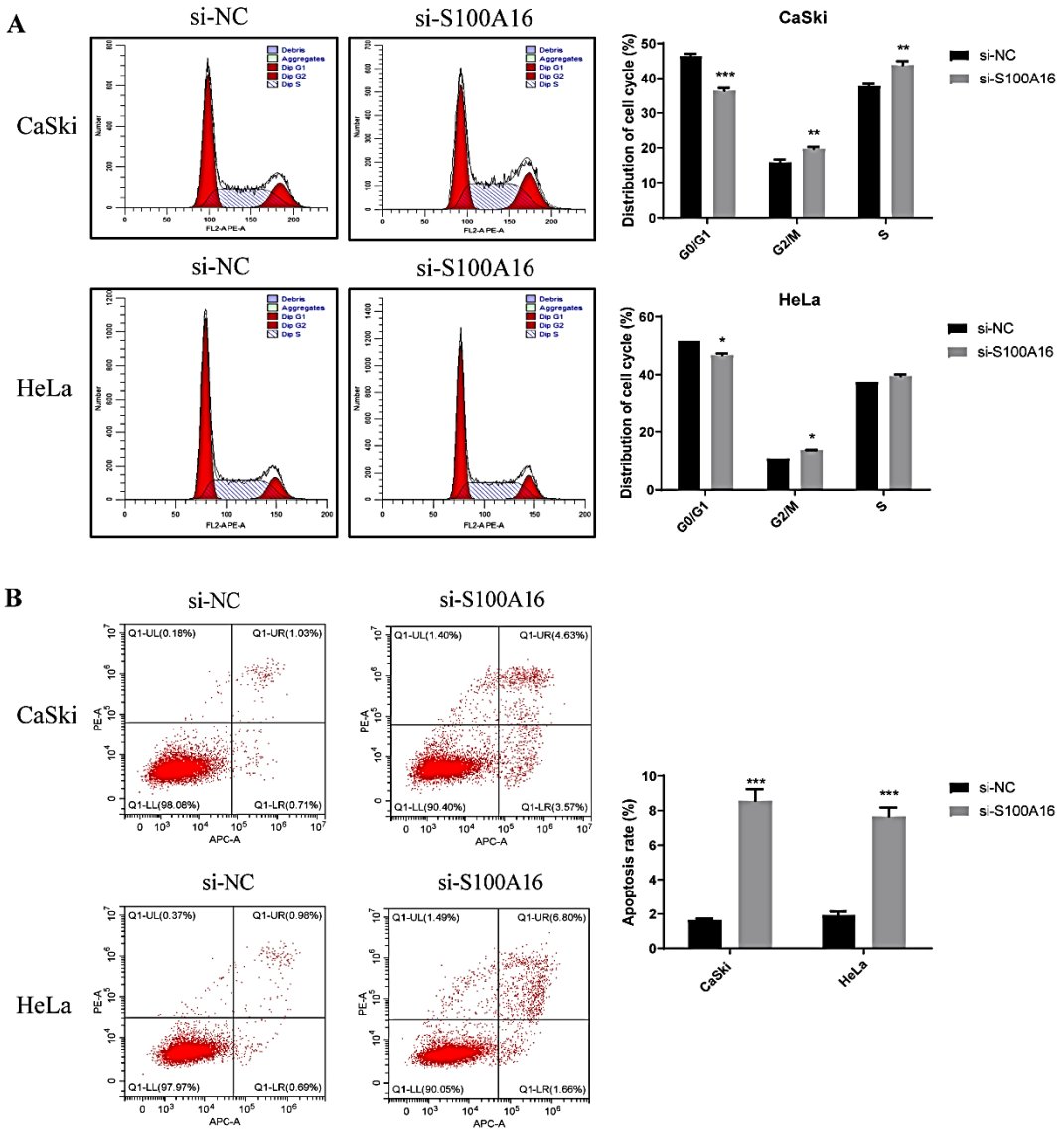

Figure 3: Effect of silencing S100A16 on biological behavior of CC cells. (A) Flow cytometry detection of cell cycle arrest in each group of cells. (B) Flow cytometry detection of apoptotic cells rate in each group. Q1-LL is normal cells, Q1-LR is early apoptotic cells, Q1-UR is late apoptotic and necrotic cells, and Q1-UL is cell debris or mechanically damaged cells. Data were shown as mean±SD (n=3). Compared with the si-NC group, $^{*}p<0.1$, $^{**}p<0.01$, $^{***}p<0.001$.

promoted the proliferation, migration, and angiogenesis of HeLa cells.[23] S100A16 may serve as a potential therapeutic target and CC tumor marker.[12] In the research, we identified the specific mechanism of S100A16 in the evolution of CC tumors. We discovered that S100A16 is substantially expressed in CC cell lines and tissue samples, indicating that S100A16 promotes CC progression. HeLa cells, the first immortalized human cell line, proliferate rapidly and are widely used in cancer research. The CaSki cell line contains a high copy number of HPV-16 viral DNA, which is highly invasive and metastatic potential, and is widely used to study the metastasis mechanism of CC. C-33A cells showed subdiploid karyotype and epithelial cell morphology, but the karyotype showed instability with successive passage. Therefore, HeLa and CaSki cell lines were chosen for further experimentation. Subsequently, *in vivo* and *in vitro* tests revealed that silencing S100A16 decreased CC development, while overexpression of S100A16 increased CC cell proliferation. We investigated the mechanism by which S100A16 operates in CC and found that it facilitates tumor growth via the PI3K/AKT/mTOR signaling pathway. In conclusion, this study fully highlighted the innovation of S100A16 as a possible therapeutic target and potential biomarker for CC.

The induction of tumor cell death has long been a primary goal in clinical oncology research. However, therapies that target programmed cell death remain highly complex. Programmed cell death can be accomplished through apoptosis and autophagy, which can work together to promote tumor cell death. To maintain cellular balance, autophagy removes damaged and potentially

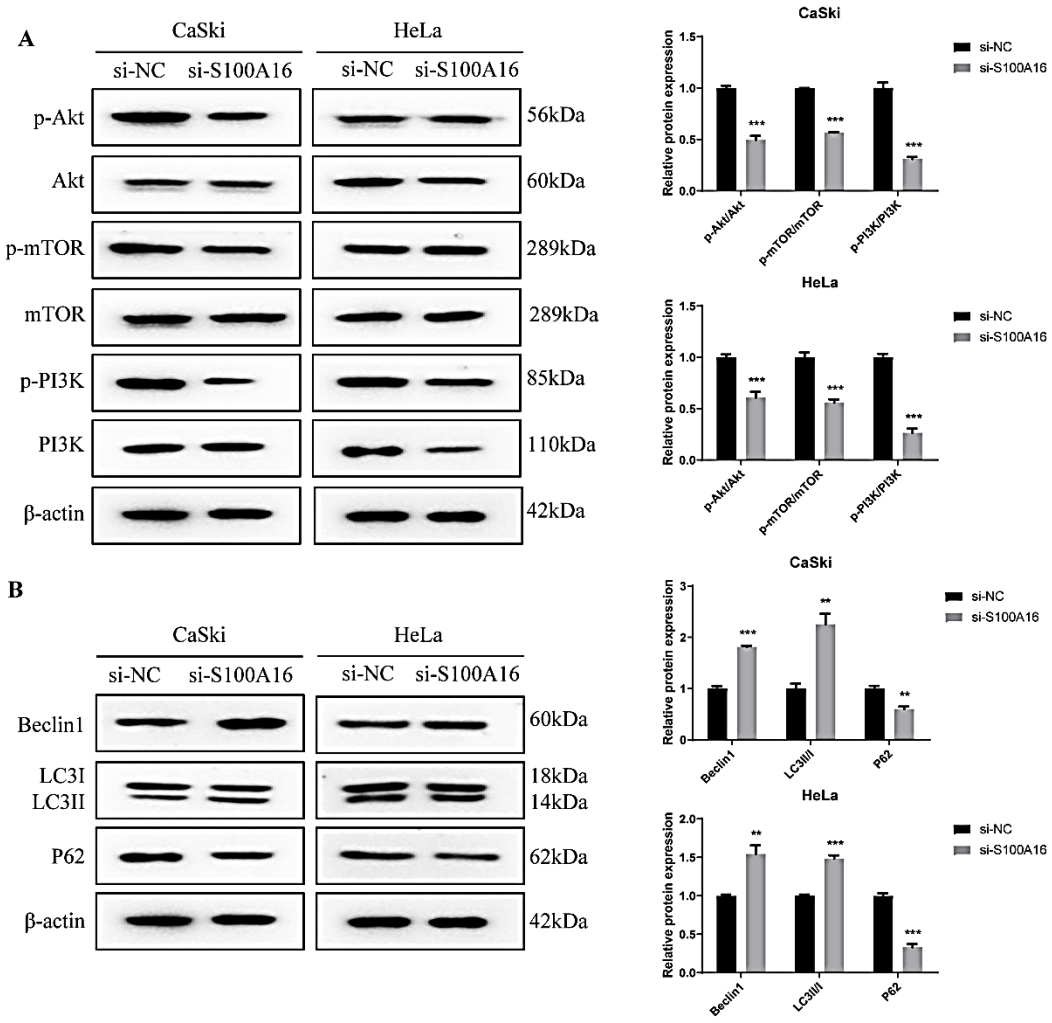

Figure 4: Effects of silencing S100A16 on the PI3K/AKT/mTOR signal pathway in CC cells. (A) The expression of p-PI3K, PI3K, p-Akt, Akt, p-mTOR and mTOR in each cell group was detected by Western blot. (B) Expression levels of LC3II/I, p62, and Beclin1 in each cell group were measured by Western blot. Data were shown as mean±SD (n=3). Compared with the si-NC group, $^{**}p$<0.01, $^{***}p$<0.001.

Table 1: CC tumor weight in all groups of mice.

	shRNA-NC	shRNA- S100A16	ov-NC	ov-S100A16
Tumor weight	1.49±0.18	0.90±0.23***	1.52±0.22	1.88±0.05$^{\#\#}$

Data were shown as mean±SD and analyzed by one-way ANOVA (n=5). Compared with the shRNA-NC group, $^{***}p$< 0.001. Compared with the ov-NC group, $^{\#\#}p$< 0.01.

Table 2: CC tumor volume in each group of mice.

Volume	shRNA-NC	shRNA- S100A16	ov-NC	ov-S100A16
4 d	46.18±20.70	12.94±15.21**	27.69±14.22	33.49±10.87
8 d	213.68±46.89	70.19±86.87*	178.51±67.21	283.88±141.33
12 d	397.18±191.49	225.32±184.32	455.01±40.10	737.37±223.96$^{\#}$
16 d	657.4±158.48	269.53±142.16**	529.96±55.03	895.81±291.89$^{\#\#}$
20 d	1191.16±401.59	527.71±253.69**	760.88±206.62	1096.98±428.51
24 d	1492.8±240.31	781.04±178.89**	1458.01±323.89	1937.72±400.34$^{\#}$

The volume was determined using the formula: V=(L×(W)^2) / 2 (V, volume; L, length diameter; W, width diameter). Data were shown as mean±SD and analyzed by one-way ANOVA (n=5). Compared with the shRNA-NC group, $^{*}p$<0.1, $^{**}p$<0.01. Compared with the ov-NC group, $^{\#}p$<0.05, $^{\#\#}p$<0.01.

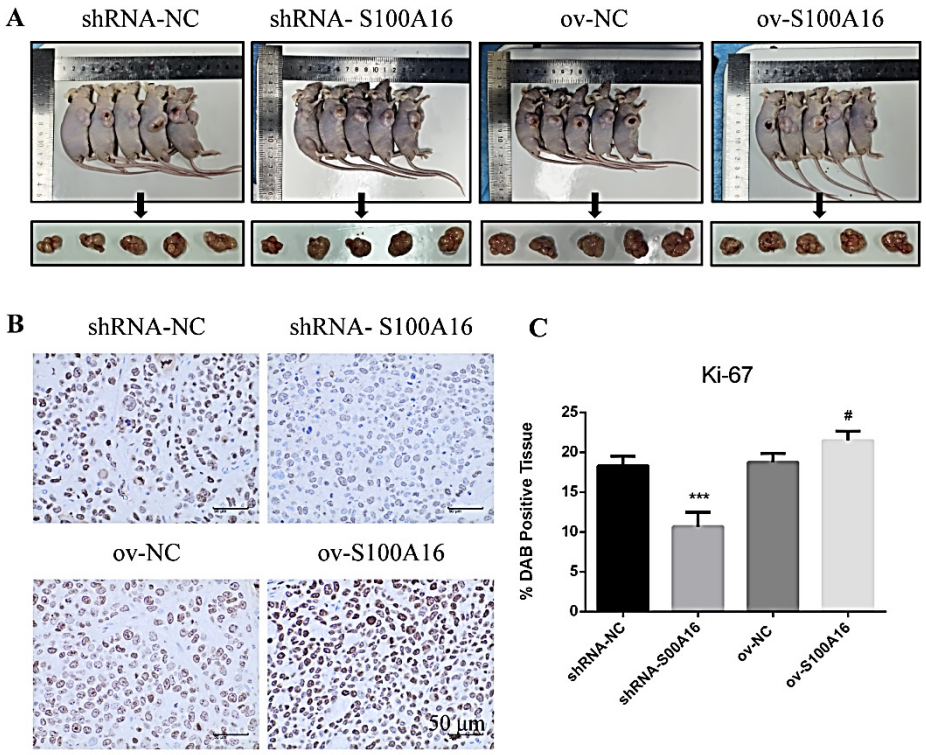

Figure 5: The subcutaneous tumor-bearing mouse model was used to detect the effect of silencing S100A16 expression on the proliferation of CC cells *in vivo*. (A) The representative images of the tumor in nude mice (n=5 each group). (B, C) Ki-67 was detected in tumor tissues by immunohistochemical staining. Data were shown as mean±SD (n=3). Compared with shRNA-NC, $^{***}p<0.001$. Compared with the ov-NC group, $^{\#}p<0.05$.

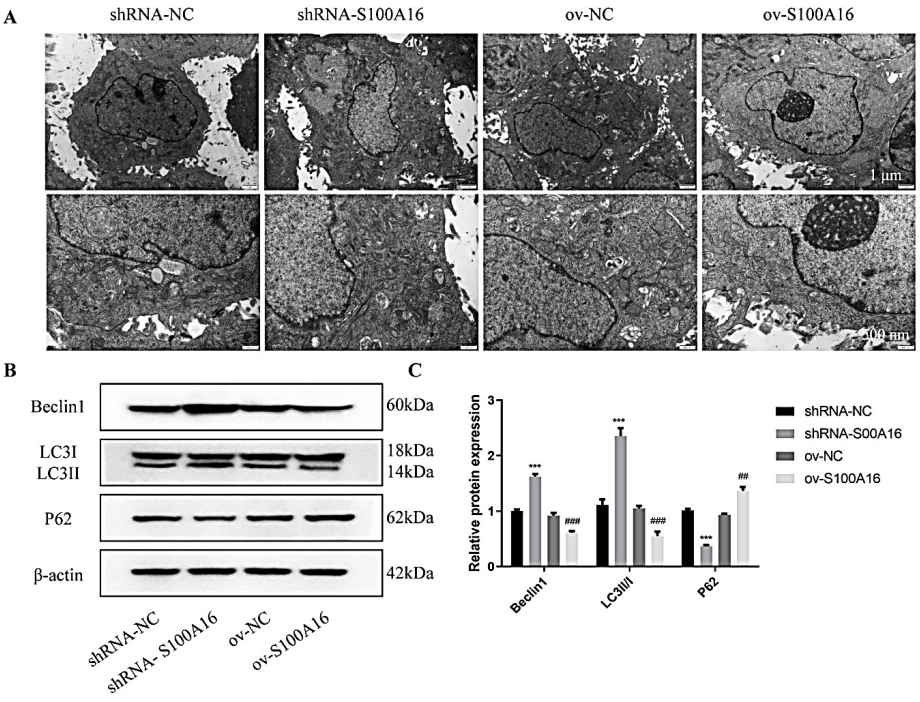

Figure 6: A subcutaneously transplanted tumor model was used to detect the effect of S100A16 expression on autophagy in transplanted tumor tissue. (A) TEM detection of tumor tissue. (B, C) Western blot was used to detect the expression of LC3II/I, p62, and Beclin1 proteins in transplanted tumor tissues. Data were shown as mean±SD (n=3). Compared with the shRNA-NC group, $^{***}p<0.001$. Compared with the ov-NC group, $^{\#\#}p<0.01$, $^{\#\#\#}p<0.001$.

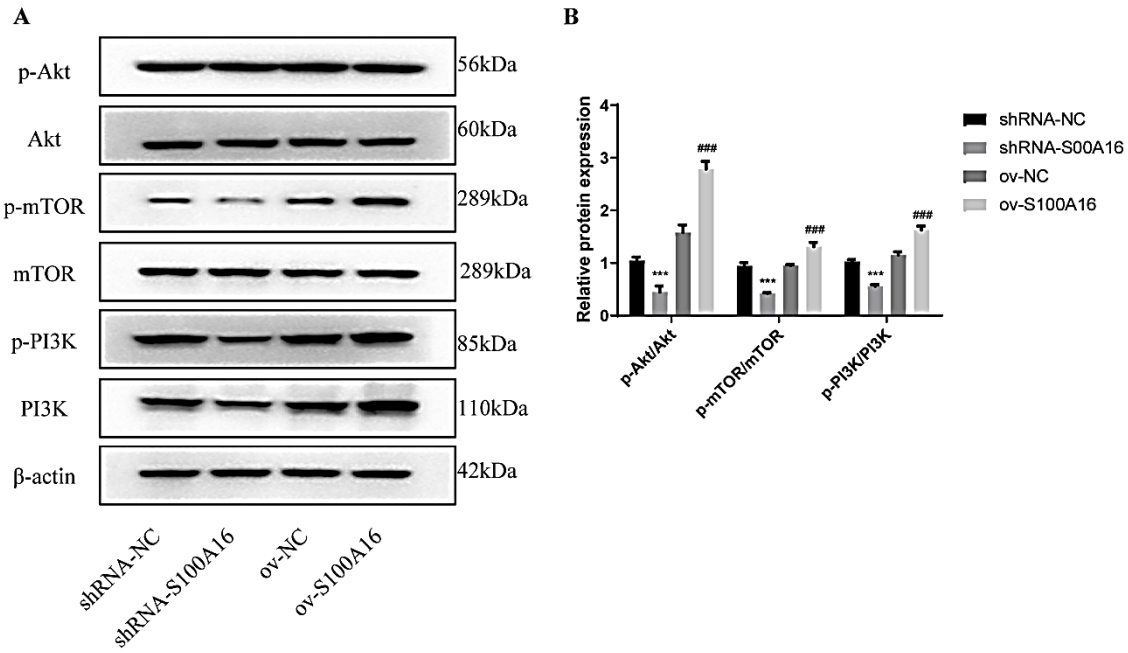

Figure 7: Effects of S100A16 expression on the PI3K/AKT/mTOR signaling pathway in the transplanted tumor tissues were detected by Western blot. (A) Representative Western blot bands. (B) Quantitative analysis of Western blot bands. Data were shown as mean±SD (n=3). Compared with the shRNA-NC group, $^{***}p<0.001$. Compared with the ov-NC group, $^{\#\#}p<0.01$, $^{\#\#\#}p<0.001$.

toxic components of the cell. Beclin1 is a well-established regulator of autophagy that has been shown to interact with other proteins to form class III PI3K complexes, thereby inducing the autophagy process.[29] Recent studies have highlighted the critical role of the autophagy-related protein LC3B in this process, where the conversion of LC3I to LC3II upon lipidation is essential for the formation and maturation of autophagosomes.[30] Additionally, p62 is a key autophagy receptor that selectively interacts with LC3 on autophagosomes, facilitating the sequestration and degradation of protein aggregates, lipid droplets, and damaged organelles.[31] Our research demonstrated that silencing S100A16 leads to an increase in the Beclin1 expression and the LC3II/LC3I ratio, while simultaneously decreasing p62 expression. These findings suggest that S100A16 may play a significant role in regulating the autophagic process, potentially influencing cellular homeostasis. Increasing evidence suggests a significant relationship between apoptosis modulation as well as autophagy activation, providing a framework for cancer treatment. The findings of this study demonstrate that suppressing S100A16 can reduce the migration and proliferation of CC cells, extend the development cycle of these cells, and increase the rate of apoptosis. This implies that inhibiting S100A16 can trigger both apoptosis and autophagy in CC cells, promoting programmed cell death. Therefore, S100A16 is anticipated to serve as a promising target for antitumor drug development.

The PI3K/AKT/mTOR pathway is involved in the occurrence and development of numerous human malignancies.[19,32] In most cancer cells, the PI3K/AKT/mTOR pathway is active.[33,34] It regulates the apoptotic response by interacting with several key players in the apoptotic process. According to studies, the PI3K/AKT signaling pathway controls CC development as well as invasion, which is vital in the onset and development of CC.[35-37] Furthermore, it is well known that the PI3K/AKT/mTOR signaling pathway plays an important role in autophagy, and autophagy is enhanced when the PI3K/AKT pathway is inhibited.[38] As a key negative regulatory axis of autophagy, mTOR can form two key complexes, mTORC1 and mTORC2, which play an important regulatory role in the autophagy response.[39] Although some inhibitors targeting the PI3K/AKT/mTOR signaling pathway are currently used in cancer treatment, there are still concerns about the possibility of drug resistance, side effects, and other adverse reactions in patients.[40] In our study, inhibition of S100A16 reduced the activity of the PI3K/AKT/mTOR signaling pathway to promote autophagy and further inhibited the proliferation, migration, and invasion of CC cells. However, overexpression of S100A16 activated the PI3K/AKT/mTOR signaling pathway, facilitating cancer cell development as well as progression. Therefore, targeting S100A16 may act as a potential PI3K/AKT/mTOR signaling pathway inhibitor to prevent CC progression.

However, there were some limitations in this study. Although the study identified the inhibitory effect of S100A16 on the PI3K/AKT/mTOR pathway, it did not investigate the regulatory interactions or downstream effects in depth. In addition, the potential effects of S100A16 silencing on non-cancer cells or the variability among cervical cancer subtypes warrant further investigation. Additionally, more in-depth evaluation of the correlation between S100A16 and clinical CC patients is needed in the future to provide a scientific basis for its use as a new

diagnostic marker or therapeutic target. Future research should also focus on developing S100A16-targeted therapies, which may offer innovative approaches to improve patient outcomes.

CONCLUSION

This study demonstrates that silencing S100A16 effectively reduces the development of CC cells, simultaneously inducing apoptosis as well as autophagy. Furthermore, S100A16 is implicated in the activation of the PI3K/AKT/mTOR signaling pathway. The suppression of S100A16 inhibits this pathway, thereby enhancing cellular autophagy. In summary, silencing S100A16 emerges as a potent inducer of autophagy and apoptosis, potentially offering novel therapeutic strategies for the treatment of CC.

FUNDING STATEMENT

The study was funded by the Natural Science Foundation of Gansu Province (22JR11RA073).

CONFLICT OF INTEREST

The authors declare that there is no conflict of interest.

ABBREVIATIONS

CC: Cervical Cancer; **PI3K:** Phosphatidylinositol 3-Kinase; **AKT:** Protein Kinase B; **mTOR:** Mechanistic Target of Rapamycin; **S100A16:** S100 Calcium-Binding Protein A16; **RT-qPCR:** Reverse Transcription Quantitative Polymerase Chain Reaction; **siRNA:** Small Interfering RNA; **si-NC:** Small Interfering RNA Negative Control; **si-S100A16:** Small Interfering RNA targeting S100A16; **CCK-8:** Cell Counting Kit-8; **DMEM:** Dulbecco's Modified Eagle Medium; **FBS:** Fetal Bovine Serum; PBS: Phosphate-Buffered Saline; **HRP:** Horseradish Peroxidase; **PVDF:** Polyvinylidene Difluoride; **BCA:** Bicinchoninic Acid; **LC3II/I:** Microtubule-Associated Protein 1A/1B-Light Chain 3 II/I; **p62:** Sequestosome 1; **ANOVA:** Analysis of Variance; **IC_{50}:** Half Maximal Inhibitory Concentration.

AUTHOR'S CONTRIBUTIONS

Haibin Zhang and Yongxiu Yang designed the program, Haibin Zhang, Wenhu Xin and Shan Zhang provided the manuscript, Caiyun Wang produced the images, and Yongxiu Yang provided the funds. All authors reviewed the manuscript.

ANIMAL ETHICAL STATEMENT

The study was approved by the Experimental Animal Ethics Committee of the Second Hospital of Lanzhou University (D2022-320).

SUMMARY

This study explores the role of S100A16 in Cervical Cancer (CC) progression, examining the effects of silencing S100A16 on cellular behaviors and pathways in CC cells. S100A16 was found to be highly expressed in CC cells. Through *in vitro* and *in vivo* experiments, silencing S100A16 led to reduced cell proliferation, migration, and increased apoptosis. Mechanistically, S100A16 silencing inhibited the PI3K/AKT/mTOR pathway, inducing autophagy and reducing tumor growth. These findings suggest that targeting S100A16 may serve as a promising therapeutic strategy for CC by modulating tumor growth through the PI3K/AKT/mTOR pathway.

REFERENCES

1. Pavone G, Marino A, Fisicaro V, Motta L, Spata A, Martorana F, *et al.* Entangled connections: HIV and HPV interplay in cervical cancer-a comprehensive review. Int J Mol Sci. 2024; 25(19): 10358. doi: 10.3390/ijms251910358, PMID 39408687.
2. Huang R, Liu Z, Sun T, Zhu L. Cervicovaginal microbiome, high-risk HPV infection and cervical cancer: mechanisms and therapeutic potential. Microbiol Res. 2024; 287: 127857. doi: 10.1016/j.micres.2024.127857, PMID 39121703.
3. Landy R, Sasieni PD, Mathews C, Wiggins CL, Robertson M, McDonald YJ, *et al.* Impact of screening on cervical cancer incidence: A population-based case-control study in the United States. Int J Cancer. 2020; 147(3): 887-96. doi: 10.1002/ijc.32826, PMID 31837006.
4. Bray F, Laversanne M, Sung H, Ferlay J, Siegel RL, Soerjomataram I, *et al.* Global cancer statistics 2022: GLOBOCAN estimates of incidence and mortality worldwide for 36 cancers in 185 countries. CA Cancer J Clin. 2024; 74(3): 229-63. doi: 10.3322/caac.21834, PMID 38572751.
5. Guo M, Xu J, Du J. Trends in cervical cancer mortality in China from 1989 to 2018: an age-period-cohort study and Joinpoint analysis. BMC Public Health. 2021; 21(1): 1329. doi: 10.1186/s12889-021-11401-8, PMID 34229639.
6. Baettig F, Vlajnic T, Vetter M, Glatz K, Hench J, Frank S, *et al.* Nivolumab in chemotherapy-resistant cervical cancer: report of a vulvitis as a novel immune-related adverse event and molecular analysis of a persistent complete response. J Immunother Cancer. 2019; 7(1): 281. doi: 10.1186/s40425-019-0742-6, PMID 31672171.
7. Low RR, Fung KY, Gao H, Preaudet A, Dagley LF, Yousef J, *et al.* S100 family proteins are linked to organoid morphology and EMT in pancreatic cancer. Cell Death Differ. 2023; 30(5): 1155-65. doi: 10.1038/s41418-023-01126-z, PMID 36828915.
8. Zhang L, Zhu T, Miao H, Liang B. The calcium binding protein S100A11 and its roles in diseases. Front Cell Dev Biol. 2021; 9: 693262. doi: 10.3389/fcell.2021.693262, PMID 34179021.
9. Wei R, Feng OQ, Hui YZ, Huang X, Ping LS. Prognostic value of the S100 calcium-binding protein family members in hepatocellular carcinoma. Biosci Rep. 2023; 43(7): BSR20222523. doi: 10.1042/BSR20222523, PMID 37133437.
10. Kobayashi M, Nagashio R, Saito K, Aguilar-Bonavides C, Ryuge S, Katono K, *et al.* Prognostic significance of S100A16 subcellular localization in lung adenocarcinoma. Hum Pathol. 2018; 74: 148-55. doi: 10.1016/j.humpath.2018.01.001, PMID 29320753.
11. Basnet S, Vallenari EM, Maharjan U, Sharma S, Schreurs O, Sapkota D. An update on S100A16 in Human Cancer. Biomolecules. 2023; 13(7): 1070. doi: 10.3390/biom1307 1070, PMID 37509106.
12. Zhang H, Yang Y, Xing W, Li Y, Zhang S. Expression and gene regulatory network of S100A16 protein in cervical cancer cells based on data mining. BMC Cancer. 2023; 23(1): 1124. doi: 10.1186/s12885-023-11574-y, PMID 37978469.
13. Jiang Y, Yu X, Zhao Y, Huang J, Li T, Chen H, *et al.* ADAMTS19 suppresses cell migration and invasion by targeting S100A16 via the NF-κB pathway in human gastric cancer. Biomolecules. 2021; 11(4): 561. doi: 10.3390/biom11040561, PMID 33921267.
14. Ou S, Liao Y, Shi J, Tang J, Ye Y, Wu F, *et al.* S100A16 suppresses the proliferation, migration and invasion of colorectal cancer cells in part via the JNK/p38 MAPK pathway. Mol Med Rep. 2021; 23(2): 164. doi: 10.3892/mmr.2020.11803, PMID 33355370.
15. You X, Li M, Cai H, Zhang W, Hong Y, Gao W, *et al.* Calcium binding protein S100A16 expedites proliferation, invasion and epithelial-mesenchymal transition process in gastric cancer. Front Cell Dev Biol. 2021; 9: 736929. doi: 10.3389/fcell.2021.736929 , PMID 34650982.
16. Sun X, Wang T, Zhang C, Ning K, Guan ZR, Chen SX, *et al.* S100A16 is a prognostic marker for colorectal cancer. J Surg Oncol. 2018; 117(2): 275-83. doi: 10.1002/jso.24822, PMID 28876468.
17. Tomiyama N, Ikeda R, Nishizawa Y, Masuda S, Tajitsu Y, Takeda Y. S100A16 up-regulates Oct4 and Nanog expression in cancer stem-like cells of Yumoto human cervical

carcinoma cells. Oncol Lett. 2018; 15(6): 9929-33. doi: 10.3892/ol.2018.8568, PMID 29928366.

18. Yu L, Wei J, Liu P. Attacking the PI3K/Akt/mTOR signaling pathway for targeted therapeutic treatment in human cancer. Semin Cancer Biol. 2022; 85: 69-94. doi: 10.1016/j.semcancer.2021.06.019, PMID 34175443.
19. Glaviano A, Foo AS, Lam HY, Yap KC, Jacot W, Jones RH, *et al.* PI3K/AKT/mTOR signaling transduction pathway and targeted therapies in cancer. Mol Cancer. 2023; 22(1): 138. doi: 10.1186/s12943-023-01827-6, PMID 37596643.
20. Wang Q, Wang B, Zhang W, Zhang T, Liu Q, Jiao X, *et al.* APLN promotes the proliferation, migration, and glycolysis of cervical cancer through the PI3K/AKT/mTOR pathway. Arch Biochem Biophys. 2024; 755: 109983. doi: 10.1016/j.abb.2024.109983, PMID 38561035.
21. Zhou J, Guo Z, Peng X, Wu B, Meng Q, Lu X, *et al.* Chrysotoxine regulates Ferroptosis and the PI3K/AKT/mTOR pathway to prevent cervical cancer. J Ethnopharmacol. 2025; 338(3): 119126. doi: 10.1016/j.jep.2024.119126, PMID 39557107.
22. Kaehler M, von Bubnoff N, Cascorbi I, Gorantla SP. Molecular biomarkers of leukemia: convergence-based drug resistance mechanisms in chronic myeloid leukemia and myeloproliferative neoplasms. Front Pharmacol. 2024; 15: 1422565. doi: 10.3389/fphar.2024.1422565, PMID 39104388.
23. Zhang H, Yang Y, Ma X, Xin W, Fan X. S100A16 regulates HeLa cell through the phosphatidylinositol 3 kinase (PI3K)/AKT signaling pathway. Med Sci Monit. 2020; 26: e919757. doi: 10.12659/MSM.919757, PMID 31894756.
24. Maejima Y, Zablocki D, Nah J, Sadoshima J. The role of the Hippo pathway in autophagy in the heart. Cardiovasc Res. 2023; 118(17): 3320-30. doi: 10.1093/cvr/cvac014, PMID 35150237.
25. Perrotta C, Cattaneo MG, Molteni R, De Palma C. Autophagy in the regulation of tissue differentiation and homeostasis. Front Cell Dev Biol. 2020; 8: 602901. doi: 10.3389/fcell.2020.602901, PMID 33363161.
26. Choi EK, Kim HD, Park EJ, Song SY, Phan TT, Nam M, *et al.* 8-methoxypsoralen induces apoptosis by upregulating p53 and inhibits metastasis by downregulating MMP-2 and MMP-9 in human gastric cancer cells. Biomol Ther (Seoul). 2023; 31(2): 219-26. doi: 10.4062/biomolther.2023.004, PMID 36782271.
27. Wang D, He J, Dong J, Wu S, Liu S, Zhu H, *et al.* UM-6 induces autophagy and apoptosis via the Hippo-YAP signaling pathway in cervical cancer. Cancer Lett. 2021; 519: 2-19. doi: 10.1016/j.canlet.2021.05.020, PMID 34161791.
28. Luo X, Jian M, Wu P, Wu Y, Ma Y, Feng N, *et al.* STIM1 promotes cervical cancer progression through autophagy activation via TFEB nuclear translocation. Cell Signal. 2025; 125: 111500. doi: 10.1016/j.cellsig.2024.111500, PMID 39489201.
29. Tran S, Fairlie WD, Lee EF. BECLIN1: Protein structure, function and regulation. Cells. 2021; 10(6): 1522. doi: 10.3390/cells10061522, PMID 34204202.
30. Hwang HJ, Kim YK. The role of LC3B in autophagy as an RNA-binding protein. Autophagy. 2023; 19(3): 1028-30. doi: 10.1080/15548627.2022.2111083, PMID 35968566.
31. Huang X, Yao J, Liu L, Chen J, Mei L, Huangfu J, *et al.* S-acylation of p62 promotes p62 droplet recruitment into autophagosomes in mammalian autophagy. Mol Cell. 2023; 83(19): 3485-3501.e11. doi: 10.1016/j.molcel.2023.09.004, PMID 37802024.
32. Nagel A, Huegel J, Petrilli A, Rosario R, Victoria B, Hardin HM, *et al.* Simultaneous inhibition of PI3K and PAK in preclinical models of neurofibromatosis type 2-related schwannomatosis. Oncogene. 2024; 43(13): 921-30. doi: 10.1038/s41388-024-02958-w, PMID 38336988.
33. Li Q, Li Z, Luo T, Shi H. Targeting the PI3K/AKT/mTOR and RAF/MEK/ERK pathways for cancer therapy. Mol Biomed. 2022; 3(1): 47. doi: 10.1186/s43556-022-00110-2, PMID 36539659.
34. Hashemi M, Mohandesi Khosroshahi E, Asadi S, Tanha M, Ghatei Mohseni F, Abdolmohammad Sagha R, *et al.* Emerging roles of non-coding RNAs in modulating the PI3K/Akt pathway in cancer. Noncoding RNA Res. 2025; 10: 1-15. doi: 10.1016/j.ncrna.2024.08.002, PMID 39296640.
35. Zhang Z, Li X, Sun H. Development of machine learning models integrating PET/CT radiomic and immunohistochemical pathomic features for treatment strategy choice of cervical cancer with negative pelvic lymph node by mediating COX-2 expression. Front Physiol. 2022; 13: 994304. doi: 10.3389/fphys.2022.994304, PMID 36311222.
36. Sun G, Zhang Q, Liu Y, Xie P. Role of phosphatidylinositol 3-kinase and its catalytic unit PIK3CA in cervical cancer: a mini-review. Appl Bionics Biomech. 2022; 2022: 6904769. doi: 10.1155/2022/6904769, PMID 36046780.
37. He Y, Sun MM, Zhang GG, Yang J, Chen KS, Xu WW, *et al.* Targeting PI3K/Akt signal transduction for cancer therapy. Signal Transduct Target Ther. 2021; 6(1): 425. doi: 10.1038/s41392-021-00828-5, PMID 34916492.
38. Hao C, Wei Y, Meng W, Zhang J, Yang X. PI3K/AKT/mTOR inhibitors for hormone receptor-positive advanced breast cancer. Cancer Treat Rev. 2025; 132: 102861. doi: 10.1016/j.ctrv.2024.102861, PMID 39662202.
39. Ballesteros-Álvarez J, Andersen JK. mTORC2: the other mTOR in autophagy regulation. Aging Cell. 2021; 20(8): e13431. doi: 10.1111/acel.13431, PMID 34250734.
40. Yu M, Chen J, Xu Z, Yang B, He Q, Luo P, *et al.* Development and safety of PI3K inhibitors in cancer. Arch Toxicol. 2023; 97(3): 635-50. doi: 10.1007/s00204-023-03440-4, PMID 36773078.

Cite this article: Zhang H, Xing W, Li Y, Xu X. Silencing of S100A16 in Cervical Cancer Cells Inhibits Cancer Cell Growth by Inducing Autophagy via PI3K/AKT/mTOR Signaling Pathway. Indian J of Pharmaceutical Education and Research. 2025;59(4):1534-45.